Eur Biophys J (1999) 28: 427–436

ARTICLE

Cyril Curtain · Frances Separovic · Katherine Nielsen
David Craik · Yong Zhong · Alan Kirkpatrick

The interactions of the N-terminal fusogenic peptide of HIV-1 gp41 with neutral phospholipids

Received: 8 June 1998 / Revised version: 18 November 1998 / Accepted: 28 December 1998

Abstract We have studied the interactions with neutral phospholipid bilayers of FPI, the 23-residue fusogenic N-terminal peptide of the HIV-1_{LAI} transmembrane glycoprotein gp41, by CD, EPR, NMR, and solid state NMR (SSNMR) with the objective of understanding how it lyses and fuses cells. Using small unilamellar vesicles made from egg yolk phoshatidylcholine which were not fused or permeabilised by the peptide we obtained results suggesting that it was capable of inserting as an α-helix into neutral phospholipid bilayers but was only completely monomeric at peptide/lipid (P/L) ratios of 1/2000 or lower. Above this value, mixed populations of monomeric and multimeric forms were found with the proportion of multimer increasing proportionally to P/L, as calculated from studies on the interaction between the peptide and spin-labelled phospholipid. The CD data indicated that, at P/L between 1/200 and 1/100, approximately 68% of the peptide appeared to be in α-helical form. When P/L=1/25 the α-helical content had decreased to 41%. Measurement at a P/L of 1/100 of the spin lattice relaxation effect on the ^{13}C nuclei of the phospholipid acyl chains of an N-terminal spin label attached to the peptide showed that most of the peptide N-termini were located in the interior hydrocarbon region of the membrane. SSNMR on multilayers of ditetradecylphosphatidyl choline at P/Ls of 1/10, 1/20 and 1/30 showed that the peptide formed multimers that affected the motion of the lipid chains and disrupted the lipid alignment. We suggest that these aggregates may be relevant to the membrane-fusing and lytic activities of FPI and that they are worthy of further study.

Key words HIV-1 fusion peptide · EPR · NMR · Solid state NMR · Circular dichroism

Abbreviations *ANTS* 8-Aminonaphthalene-1,3,6-trisulfonic acid sodium salt · *CD* Ultraviolet circular dichroism spectroscopy · *CrOx* Chromium oxalate · *DPX p*-Xylene-bis(pyridinium) bromide · *DSS* 4,4-Dimethyl-4-silapentane-1-sulfonate · *DTPC* Ditetradecyl phosphatidylcholine · *EPR* Electron paramagnetic resonance spectroscopy · *EYPC* Egg yolk phosphatidylcholine · *FPI* 23-residue N-terminal fusion peptide of human immunodeficiency virus type 1 · *$FP1_a$* FPI ^{13}C carbonyl-labelled on Gly-529 · *FPII* FPI spin-labelled at N-terminus · *FT-IR* Fourier transform infrared spectroscopy · *HIV-1* Human immunodeficiency virus type 1 · *Me_2SO* Dimethylsulphoxide · *NBD-PE* N-(7-Nitro-2,1,3-benzoxadiol-4-yl)phosphatidylethanolamine · *P/L* Peptide/lipid · *RET* Resonance energy transfer · *Rh-PE N*-(Lissamine rhodamine B sulfonyl)phosphatidylethanolamine · *SDS* Sodium dodecyl sulfate · *SSNMR* Solid-state NMR spectroscopy · *SUV* Small unilamellar vesicles · *TCC* Tempocholine chloride · *TFE* Trifluoroethanol · *5NS* 5-Doxylstearic acid spin probe · *7NS* 7-Doxylstearic acid spin probe · *9NS* 9-Doxylstearic acid spin probe · *10NS* 10-Doxylstearic acid spin probe · *12NS* 12-Doxylstearic acid spin probe · *16NS* 16-Doxylstearic acid spin probe · *16NPC* 1-Palmitoyl-2-(16-doxylstearoyl) phosphatidylcholine

C. Curtain (✉) · Y. Zhong
Department of Physics, Monash University,
Clayton, Victoria 3168, Australia
e-mail: ccurtain@vaxc.cc.monash.edu.au

F. Separovic
School of Chemistry, University of Melbourne,
Parkville, Victoria 3052, Australia

K. Nielsen · D. Craik
Centre for Drug Design and Development, Gerhmann Laboratories,
University of Queensland, Queensland 4072, Australia

A. Kirkpatrick
CSIRO Division of Molecular Science, Parkville, Victoria 3052,
Australia

Introduction

The 23-residue N-terminal sequence of the gp41 envelope glycoprotein of HIV-1 is regarded as playing a key part in fusion of the viral lipid envelope and the target cell membrane because site-directed mutagenic replacement of hydrophobic residues in this sequence with polar residues re-

duces infectivity of the virus and its ability to promote syncytia formation between cultured cells (Felser et al. 1989; Freed et al. 1990). Also, peptides consisting of all or part of this sequence bind to and perturb artificial membranes, causing fusion and contents leakage in negatively charged and neutral lipid vesicles (Rafalski et al. 1990; Nieva et al. 1994; Martin et al. 1996; Pereira et al. 1997) and increasing the conductance of bilayer (black) lipid membranes (Slepushkin et al. 1992). Further, the 23-residue peptide is lytic for human erythrocytes and HUT78 cells (Mobley et al. 1992) and is fusogenic for erythrocytes (Mobley et al. 1995).

Because of its hydrophobic nature it has been assumed that the fusion peptide interacts primarily with the lipids of the cell membrane and a number of studies have been made using synthetic peptides and phospholipid vesicles of defined composition. Initially, these biophysical studies used the HIV-1_{LAI} fusion peptide, which has a positive charge at its C-terminus owing to an Arg residue at position 538, and focused on systems containing negatively charged phospholipids, primarily because there was little evidence for fusogenic activity with other kinds of lipids (Rafalski et al. 1990; Nieva et al. 1994). Further, it appeared that if the Arg were replaced with Ala the peptide was poorly fusogenic (Rafalski et al. 1990). However, there is evidence that, under some conditions, the HIV-1_{LAI} peptide is cabable of fusing and inducing leakage in neutral lipids (Martin et al. 1996; Pereira et al. 1997). Because negatively charged phospholipids most commonly occur in the cytoplasmic face of the cell membrane while the exoface consists of neutral and positively charged phospholipids (Rothman and Lenard 1977; Op den Kamp 1979), the interaction of the fusion sequence with neutral lipids would be expected to be an important step in its fusion and lysis of cells.

The exact nature of the fusogenic structure of the peptide is still uncertain. The first 16 residues of the sequence have been shown to form an α-helix by CD and FT-IR spectroscopy (Rafalski et al. 1990; Gordon et al. 1992) and high-resolution NMR in a variety of micellar and lipid vesicle systems (Chang et al. 1997). On the other hand, extended β-structure of the sequence has also been reported in lipid systems and claimed to be the fusogenic form (Nieva et al. 1994; Pereira et al. 1997). Increasing β-structure was observed (Gordon et al. 1992) with increasing peptide/lipid ratio (P/L) in SDS (CD spectroscopy) and in liposomes made from red cell ghost lipids (FT-IR). Studies made with fusion peptide spin-labelled at the N-terminus (Gordon et al. 1992) suggested that it formed aggregates in red cell ghost membranes and liposomes made from red cell ghosts at quite low P/L (> 1/1000). Significant aggregation was present at P/L values where haemolysis (Mobley et al. 1992) and fusion of resealed red cell ghosts (Mobley et al. 1995) have been observed.

These studies on the interaction of the peptide with membranes appear to have been made under fusing, lytic or indeterminate conditions and the timescale of the measurements was such that the membranes were approaching their final state of fusion or lysis. It was, therefore, unclear whether the observed structures and states of association of the peptide reflected those occurring under the initial conditions of peptide/lipid interaction, rather than the final state. Further, the studies on aggregation were made using a spin-labelled peptide, which could be open to the objection that the presence of the label may be contributing to the aggregation. Here, we report the results of spectroscopic studies on the interaction of the HIV-1_{LAI} peptide with neutral lipids under non-fusing and non-lytic conditions. These studies include solid state NMR (SSNMR) of the non-spin-labelled peptide in aligned lipid multilayers.

Materials and methods

Spin probes and lipids

Stearic acid probes, doxyl spin-labelled at the 5 (5NS), 7 (7NS), 9 (9NS), 10 (10NS), 12 (12NS) and 16 (16NS) positions, and the non-membrane-penetrant probe tempocholine chloride (TCC) were obtained from Molecular Probes, Junction City, Ore. The spin-labelled phospholipid 1-palmitoyl-2-(16-doxylstearoyl)phosphatidylcholine (16NPC) was obtained from Avanti Polar Lipids, Pelham, Ala. Spin probes from both sources were checked for purity and to ensure that their number of spins/M were > 90% of theory (Gordon and Curtain 1988). Egg yolk phosphatidylcholine (EYPC, Type XVI-E) was obtained from Sigma St Louis, Mo, and used without further purification. The ether-linked phospholipid ditetradecylphosphatidylcholine (DTPC) (Ruocco et al. 1985) was the kind gift or Dr. Mahendra Jain. The fluorescent probes *N*-(7-nitro-2,1,3-benzoxadiol-4-yl)phosphatidylethanolamine (NBD-PE) and *N*-(lissamine rhodamine B sulfonyl)phosphatidylethanolamine (Rh-PE) were purchased from Avanti Polar Lipids (Birmingham, Ala). The other fluorescent probe used, 8-aminonaphthalene-1,3,6-trisulfonic acid sodium salt (ANTS), and the quencher, *p*-xylylenebis(pyridinium)bromide (DPX), were from Molecular Probes, Junction City, Ore.

Peptides

A peptide (FPI) corresponding to the fusion sequence of HIV-1_{LAI} (NH_2-AVGIGALFLGFLGAAGSTMARS-$CONH_2$, residues 517–539 numbered according to Myers et al. 1995) was synthesised by the Merrifield solid phase synthesis method and purified on a Vydac C18 column and assayed for purity as described previously (Mobley et al. 1992). Another peptide of the same sequence as FPI (FPI_a), 99% ^{13}C labelled on the carbonyl C of Gly-529 was prepared, purified and assayed by the same methods. A spin-labelled version of FPI (FPII) labelled at the N-terminus was prepared as described previously (Gordon et al. 1992). Stock solutions of the peptides in either Me_2SO or TFE/ H_2O (60/40) were used within 5 days of preparation.

Vesicle preparation

Small unilamellar vesicles (SUV) were prepared by hydrating dried EYPC in pH 7.4, 0.05 M Tris buffered solutions to a final concentration of 100 mM and sonicating under nitrogen at 35 °C until the suspension was no longer turbid. The peptides were incorporated into the vesicles by mixing them with the phospholipid in excess 70/30 chloroform/methanol at the desired peptide/lipid ratio. The mixture was dried under a stream of nitrogen and then kept under vacuum for 24 h to ensure thorough removal of solvent. The mixture was then hydrated in pH 7.0, 0.05 M Tris-HCl buffer and sonicated as above.

Density gradient centrifugation

Density gradient centrifugation of SUV was carried out in Metrizamide (Nyegaard, Oslo, Norway)-Tris buffer (pH 7.0, 0.05 M) as described by Cornell et al. (1988).

Fluorimetric assays

A Perkin Elmer MP5 spectrofluorimeter was used and measurements were made at 303 K in thermostated cuvettes.

Membrane mixing assays

The resonance energy transfer (RET) assay of Struck et al. (1981) was used to detect fusion of SUV and mixing of their membrane components. SUV whose lipid bilayers contained 0.6 mol% each of NBD-PE and Rh-PE were mixed with unlabelled SUV. On the addition of a fusogen, which mixes the labelled and unlabelled lipids, the dilution of the fluorochrome results in an increase of NDB fluorescence as measured at 530 nm with the excitation set at 465 nm. Values were expressed as a percentage of the emission obtained after the mixed SUV were exposed to 1% (w/v) Triton X-100.

Contents leakage

The ANTS/DPX assay of Ellens et al. (1985), which depends on relief of quenching as the DPX is diluted in the external medium, was used to measure the release of vesicular contents. SUV were made which encapsulated 12.5 mM ANTS, 45 mM DPX, 20 mM NaCl and 5 mM HEPES. The SUV were separated from unencapsulated material by gel filtration in a Sephadex G-75 column, eluted with 5 mM HEPES and 100 mM NaCl (pH 7.4). Osmolalities were adjusted with the aid of cryoscopic determination (Nieva et al. 1994). The ANTS fluorescence was measured at 520 nm, using an excitation of 355 nm. Readings were expressed as a percentage of the value obtained after the SUV were mixed with 1% (w/v) Triton X-100.

CD spectra

Far-ultraviolet CD spectra of FPI in TFE/H_2O (60/40) and SUV were measured over the range 250 nm to 200 nm using an AVIV spectropolarimeter at 309 K using 0.01 or 0.05 cm pathlength rectangular quartz cells. The peptide was added over a range of concentrations to SUV (2 mg lipid/ml) in 50 mM potassium monohydrogen phosphate-100 mM NaCl. Peptide concentration in the sample solution was measured by quantitative amino acid analysis. Thirty six spectra were averaged, the SUV spectra baseline-corrected by subtracting the spectra for SUV without peptide and all were analysed for % α-helix, β-strand and disordered structures using the K2d Kohonen neural network program (Andrade et al. 1993; Merelo et al. 1994) obtainable by ftp anonymous to swift.embl-heidelberg.de directory/group/andrade.

Magnetic resonance spectroscopy

Nuclear magnetic resonance

Solution ^{13}C NMR spectra were recorded at 303 K on a Bruker AMX 300 spectrometer operating at 75 MHz and chemical shifts were referenced to DSS. T_1 experiments were performed using the fast inversion-recovery (FIRFT) method (Levy et al. 1980). A recycle delay of 1.3 s was incorporated between each 180°-τ-90° pulse sequence and a set of 12 τ values was used to determine T_1 values. All spectra were recorded in 16 k data points with a spectral width of 20 000 Hz and 768 transients. Spectra were processed on a Silicon Graphics workstation using the software package FELIX (Hare Research). Each free induction decay was multiplied by an exponential function, leading to a line broadening of 2 Hz. A polynomial baseline correction of order 2 was applied to each transformed spectrum. Raw peak intensities were input into KALEIDOGRAPH where T_1 values were calculated using a 3 parameter fit. The calculated T_1 values represent an average of two determinations for each sample that were reproducible within 15%. T_1 values were determined for the phospholipid acyl chain carbon atoms in SUV into which had been incorporated FPII at a P/L of 1/100. The observed relaxation time T_1^{Obs} in these experiments is a multi-component term with contributions arising in principle from dipolar (T_1^D), paramagnetic (T_1^P), spin rotation (T_1^{SR}) and scalar coupling (T_1^{SC}) relaxation mechanisms. For protonated carbons the dipolar mechanism generally dominates the observed relaxation time and other mechanisms can be neglected. The effect of adding a paramagnetic centre, such as a nitroxide spin label, is to enhance the relaxation of those carbon atoms in the vicinity of the unpaired electron by virtue of the increased significance of $1/T_1^P$.

Solid state NMR

Proton-enhanced ^{13}C and ^{31}P SSNMR spectra were obtained at 303 K on both powder and aligned multilayers of

FPI_a dispersed in the ether-linked phospholipid DTPC with a Bruker MSL400 spectrometer using the procedures described by Cornell et al. (1988). The peptide and lipid (30–50 mg) were co-dispersed in $CHCl_3$/MeOH (approx. 1 ml) and syringed onto small glass coverslips (30–50). The solvent was allowed to evaporate and the samples were pumped overnight to remove all traces of solvent. About 1–2 µl of water was added to each of the coverslips, which were then stacked and inserted in a NMR sample tube containing 10–15 µl of water. The tube was then glass sealed. The final water concentration was 50% w/w. The ^{13}C proton-enhanced cross-polarisation sequence of Pines et al. (1973) was used. Typical conditions were: Hartmann-Hahn 90° pulse 8 µs, repetition delay 2 s, contact time 1.5 ms, acquisition time 8.5 ms, sweep width 60 kHz, 50 000 acquisitions per spectrum, obtained in lots of 2 000. The sample was goniometer-mounted to permit rotation through an angular range of 180° to 0° to the B_0 field without removing the probe from the spectrometer. ^{31}P spectra were obtained using both cross polarisation and proton decoupling. Relaxation measurements were made using an inversion-recovery (180-τ-90) sequence for T_1 and a spin-echo (90-τ-180) sequence for T_2. $T_{1\rho}$ was measured using a proton spin locking pulse. $T_{1\rho}$ is T_1 in the rotating frame or T_1 on the timescale of the spin-locking pulse (kHz) and hence reports on motion on a slower timescale.

Electron paramagnetic resonance

Continuous-wave X-band EPR spectra were obtained on Bruker ED200 and ESP380 spectrometers. Samples (25 µl) were drawn into 100 µl micropipettes and handled as described by Gordon and Curtain (1988) to ensure reproducibility. The EPR measurements were made at a significantly lower temperature (295 K) than the other spectroscopic determinations in order to ensure better resolution of the partially immobilised component in the experiments using spin-labelled lipid. At this temperature the hydrocarbon chains of the EYPC would still be in the liquid crystalline phase. In series of spectra, where subtractions were made, *x*-axis reproducibility was further ensured by including in the samples a small amount of the water soluble, non-membrane penetrant spin probe TCC to the samples. Reproducibility of addition was ensured by incorporating TCC in the stock buffer used to suspend the liposomes. This probe gave a sharp triplet spectrum, which enabled alignment of the spectra to within 0.2 G. Since TCC was added in a constant amount, it also acted as an internal standard, enabling the relative number of spins in each sample to be determined with a precision of 2%. Spin labelled peptide was added to SUV as described by Gordon et al. (1992). The fatty acid spin probes were added as concentrated ethanolic solutions. The final ethanol concentration was always below 0.25% at which there was no effect on the EPR spectrum (Ellena et al. 1983). To avoid line-broadening effects due to fatty-acid probe aggregation at high probe/lipid (Gordon and Curtain 1988), P/L ratios were kept below 1/600, except where otherwise mentioned. The phospholipid spin probe (16NPC) does not tend to aggregate to the same extent as the nitroxide fatty acids and was used at 1/300. Because this probe does not partition quantitatively into SUV when added in solvent, it was added when the phospholipid and phospholipid peptide mixtures were made up in chloroform/methanol.

Measurement of spectral parameters was carried out using Bruker Winepr and spectra were simulated with Bruker SimFonia. Where spin label motion is predominantly isotropic, a rotational correlation time (T_R) provides an empirical parameter sensitive to motion in the region probed by the spin label (Keith et al. 1974):

$$\tau_R = 6.5\times10^{-10}\times DH_0\,[(h_0/h_{-1})^{1/2}-1]\ \text{s} \quad (1)$$

where DH_0 is the mid-field line width and h_0 and h_{-1} are the amplitudes of the mid- and high-field lines, respectively. Equation (1) is valid for approximately $\tau_R = 10^{-10}$ s.

Where the labels exhibited rapid anisotropic motion and restricted flexibility, the order parameter *S* was used to assess flexibility:

$$S = (\boldsymbol{T}_{\parallel}-\boldsymbol{T}_{\perp})\times a_N/(\boldsymbol{T}_{zz}-\boldsymbol{T}_{xx})\times a'_N \quad (2)$$

where $\boldsymbol{T}_{\parallel}$ and $\boldsymbol{T}_{\perp}$ are the hyperfine tensors experimentally determined from the inner and outer hyperfine splittings, $\boldsymbol{T}_{xx}$ = 6.1 G, $\boldsymbol{T}_{zz}$ = 32.4 G are the principal elements of the real hyperfine splitting tensor in the spin Hamiltonian of the probe system, which can be measured from single-crystal EPR spectra, while a_N and a'_N are the isotropic hyperfine coupling constants for the probe. Respectively, $a_N = 1/3\times(\boldsymbol{T}_{\parallel}+2\,\boldsymbol{T}_{\perp})$ G and $a'_N = 1/3\times(\boldsymbol{T}_{zz}+2\,\boldsymbol{T}_{xx})$ G. Because it is sensitive to the polarity of the environment of the probes, the value of a_N was used as an index of their penetration into the bilayer of the SUV.

The analysis of EPR spectra of peptide/lipid mixtures was carried out using the spectral subtraction and addition methods described by Marsh (1989). As a check on the validity of these procedures as applied to our system, the lipid spin label spectra were simulated using the modified Bloch equations as described by Davoust and Devaux (1982). The rate of change of magnetisation due to exchange between the motionally restricted and fluid sites is given by the expressions

$$dM_b/dt = -\tau_b^{-1}M_b + \tau_f^{-1}M_f \quad (3)$$

$$dM_f/dt = \tau_b^{-1}M_b - \tau_f^{-1}M_f \quad (4)$$

where M_b and M_f are the spin magnetisations associated, respectively, with the "bound" and "fluid" spin label populations and τ_b^{-1} and τ_f^{-1} are the probabilities per unit time of transfer from the "bound" to the "fluid" state and vice versa. Equations (3) and (4) were incorporated into the Bloch equations for the response of the spin system to the microwave magnetic field H_1 of angular frequency ω. In the simulations, Model I of Davoust and Devaux (1982) was used, where the unique director orientation in the fluid component corresponding to the nitroxide axes being aligned along the membrane normal in the motionally restricted component was assumed to be preserved on exchange.

Results and discussion

Density gradient centrifugation

SUV made from EYPC co-solvated with FPII (25 ml) were layered onto a preformed Metrizamide gradient and centrifuged at 15 000 *g* for 3 h. As a control, 25 ml of a 0.5% (w/v) solution of FPII was centrifuged under identical conditions. One ml fractions were collected and the distribution of FPII in each of the fractions was determined by double integrating its EPR spectrum and calculating the number of spins. In the control, all the FPII was found in a band corresponding to a density range of 1.11–1.14. In the liposome preparations, at a P/L of both 1/500 and 1/100, 95% of the peptide was associated with the opalescent band of liposomes that formed at the top of the tube at a density of 1.03–1.05. The experiment was repeated with FPII being added to SUV at nominal P/Ls of 1/500 and 1/100 from TFE/H_2O (60/40) solution and it was found that 75–90% of the spin label was associated with the density band corresponding to the liposomes, but only 1–4% was in the density band 1.11–1.14. The balance of the label was found adhering to the polypropylene tube walls, from which it could be recovered in Me_2SO. This finding is in accord with that of Nieva et al. (1994) who found that substantial but varying amounts of the HIV-1 fusogenic peptide did not penetrate the membrane but was dispersed as insoluble aggregates in the aqueous phase. In our case, most of this material was adsorbed to the hydrophobic walls of the sample tube. For this reason, whenever quantitative P/L values were required we added FPI to the liposomes by initially co-solvating it with the lipid since the above results indicated that, over the concentration range studied, most of the peptide incorporated in this way was associated with the liposomes. On the other hand, FPII was added from TFE/H_2O (60/40) because it was possible to calculate concentrations from its EPR spectra.

Contents leakage and fusion

The data from the contents leakage and fusion experiments carried out at P/L ranging from 1/20 to 1/100 are given in Fig. 1A and B. It can be seen that, at the temperature employed, FPI has very little fusogenic and pore-forming activity in the SUV. Pereira et al. (1997) reported that FP1 was fusogenic for large unilamellar vesicles (LUV) made from neutral lipids comprising phosphatidylcholine, phosphatidylethanolamine and cholesterol (molar ratio 1:1:1) which selected for an extended structure that became fusogenic in a dose-dependent fashion. At sub-fusogenic doses this structure caused the release of trapped fluorochrome from LUV, indicating the existence of a peptide-mediated membrane destabilising process before and independent of the development of fusion. FPI may have been non-fusogenic or leakage-inducing for our SUV because their tighter radius might have precluded penetration of the peptide to the inner leaflet of the bilayer. Regardless of the mechanism, we considered the SUV to be a suitable medium for studying the interaction of FPI with neutral lipids under non-fusing conditions.

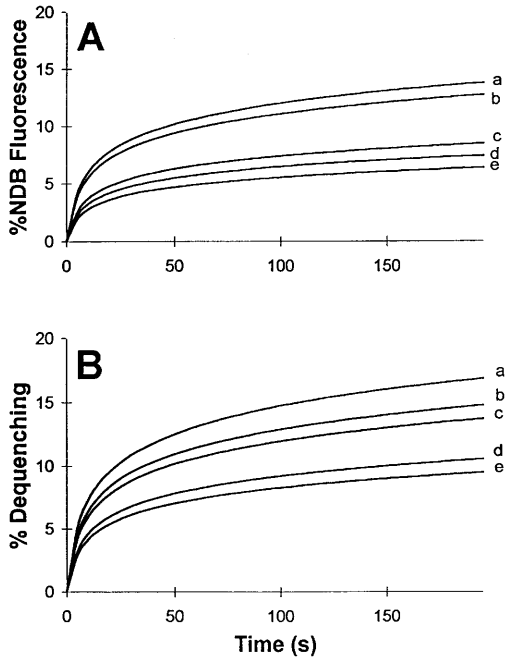

Fig. 1 **A** Fusion of SUV in the presence of FPI. Lipid mixing determined by the RET assay as a function of time and peptide to lipid ratio. Vesicle concentration in all runs was 50 μM. Fluorescence was recorded continuously with a time constant of 2.5 s. FP1/lipid ratios are: curve *a* 1/20, *b* 1/40, *c* 1/60, *d* 1/100, *e* vesicles with no FP1. **B** FPI-induced leakage of ANTS/DPX from SUV. Vesicle concentration in all runs was 50 μM. As in **A**, fluorescence was recorded continuously with a time constant of 2.5 s. FP1/lipid ratios are: curve *a* 1/20, *b* 1/40, *c* 1/60, *d* 1/100, *e* vesicles with no FP1

Circular dichroism spectroscopy

Figure 2 shows spectra of FPI dissolved in TFE/H_2O (60/40) and dispersed in SUV at P/Ls of 1/200, 1/100, 1/75 and 1/50. The proportions of each conformation for each spectrum are given in Table 1. The data indicate that the peptide has a considerable amount of helical structure in both the structure-promoting solvent TFE/H_2O (60/40) and the SUV, with the % helix decreasing with increasing concentration of peptide in the phospholipid, as had been observed previously in SDS and red cell ghost lipids (Gordon et al. 1992).

It is possible to argue on theoretical grounds (Brasseur et al. 1988, 1990; Gordon et al. 1992) that, in the presence of lipid, the amphiphilic part of the molecule from the N-terminus to Gly532 can form a α-helix. This has recently been confirmed by an NMR study (Chang et al. 1997). That is to say, the maximum theoretical α-helical content of the fusion peptide would be 66% on a residue basis. Hence, within the margins of experimental error, the 69% α-helix that we observed at a P/L of 1/200 suggests that close to 100% of the molecules were in this form at lower P/Ls.

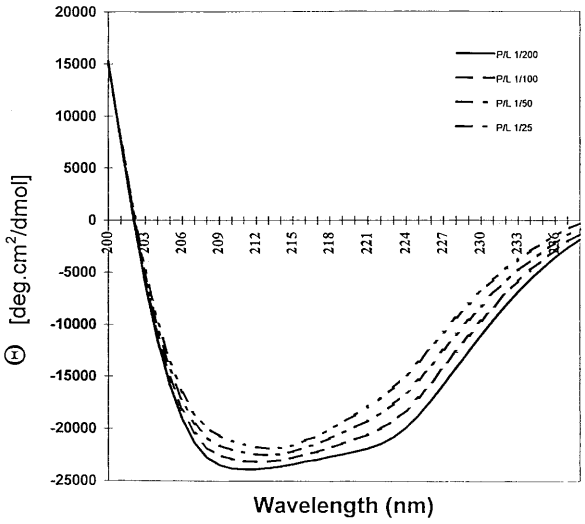

Fig. 2 Circular dichroism spectrum of FPI in SUV at peptide/lipid ratios of 1/200, 1/100, 1/75 and 1/50. Each curve is signal-averaged from 36 spectra, each collected with a sweep time of 120 s and a time constant of 1 s

Table 1 Conformations of FPI at different P/L in EYL SUV as calculated from the circular dichroism spectra in Fig. 1 using the K2d program

P/L	α-Helix (%)	β-Strand (%)	Random (%)	Correlation coefficient
1/200	69	16	15	0.928
1/100	63	24	13	0.911
1/50	51	33	16	0.943
1/25	41	44	15	0.926

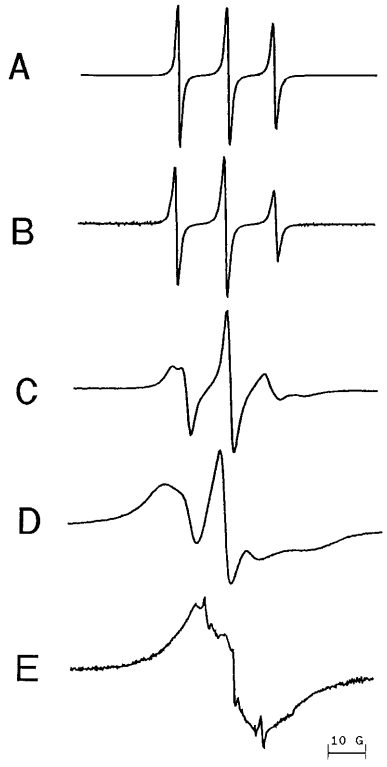

Fig. 3 EPR spectra of free spin label (*A*) and the amino-spin-labelled peptide (FPII) in TFE/H_2O (60/40) (*B*) and (FPII) in EYPC SUV (100 mg lipid/ml) at peptide/lipid ratios of 1/2000 (*C*), 1/500 (*D*) and 1/100 (*E*). Mid-field of the spectra is 3350 G. The spectra were recorded at 295 K using a microwave power of 5 mW, a modulation amplitude of 2 G, a sweep time of 2 min and a time constant of 100 ms

Only at a P/L of 1/25 does the proportion of β-strand reach a very high level. This is in contrast to the finding by Pereira et al. (1997) that the FT-IR spectra of FP1 associated with phosphatidylcholine, phosphatidylethanolamine and cholesterol (molar ratio 1:1:1) showed a high level of extended structure which remained essentially constant over a P/L range 1/50–1/800.

Magnetic resonance measurements

Electron paramagnetic resonance

In Fig. 3 the EPR spectra at 295 K of the free label 3-[-(2-maleimidoethyl)carbamoyl]-2,2,5,5-tetramethyl-1-pyrrolidinyloxyl (A) and FPII (B) in TFE/water (60/40) are compared with the spectra of FPII in the SUV at P/L of 1/2000 (C), 1/500 (D) and 1/100 (E). The spectrum of the free label in the solvent indicates that it is undergoing rapid isotropic motion and the FPII spectrum shows that its motion when attached to the rigid α-helix of the peptide is rather less rapid. The values of T_R for the free and peptide bound label in the solvent were 2.5 and 7.6×10^{-10} s, respectively. In the presence of SUV at the P/L of 1/2000 the label at the N-terminus of FPII undergoes rapid anisotropic motion, the value of *S* being 0.556. At higher P/Ls of 1/500 and 1/100 the spectra show extensive exchange-broadening, suggesting aggregation of the peptide.

A comparison of the hyperfine coupling constants derived from the FPII spectrum and from the spectra of 5NS, 7NS, 9NS, 10NS, 12NS and 16NS (Fig. 4) indicates that the positions in the lipid bilayer of the 10- and 12-nitroxide probes most closely reflect that of the FPII label. The aqueous, non-membrane-penetrant broadening agent CrOx (Altenbach and Hubbel 1988) present at 0.1 M for up to 60 min had no effect on the spectra of FPII at P/Ls of 1/2000 and 1/500, indicating that none of the N-terminal label was exposed to the aqueous medium at lower P/L. At P/L of 1/100 , however, such exposure reduced the amount of label in the SUV by 60%, giving a spectrum similar to that in Fig. 3D. This result suggests that a significant amount of the peptide at high P/L is exposed to the medium. The sharp peaks visible in the exchanged-broadened spectrum in Fig. 3E would represent this exposed peptide.

The localisation of the N-terminal spin label of FPII in the bilayer hydrophobic core accords with earlier observations on the localisation of the peptide in red cell ghost membranes and liposomes made from red cell ghost lipids (Gordon et al. 1992). Recent NMR, EPR and fluorescence studies (Chang et al. 1997) have confirmed these observa-

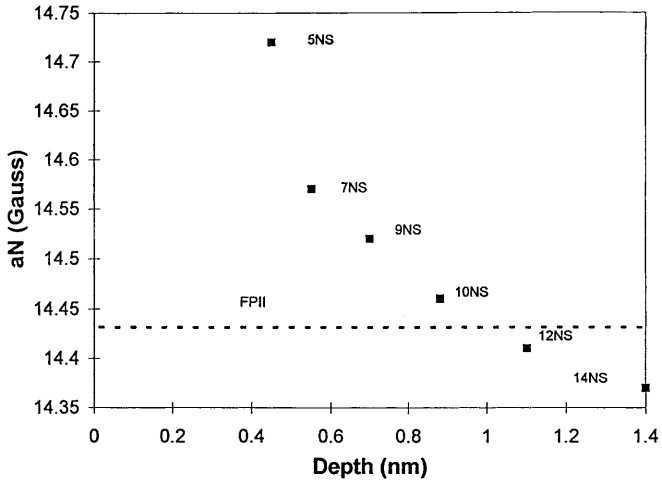

Fig. 4 Isotropic hyperfine splitting a_N of doxyl fatty acids, 5NS, 7NS, 9NS, 10NS, 12NS and 16NS, plotted against depth of insertion in the bilayer of EYPC SUV. The value of a_N for the spin-labelled peptide FPII is shown as a *dotted line*

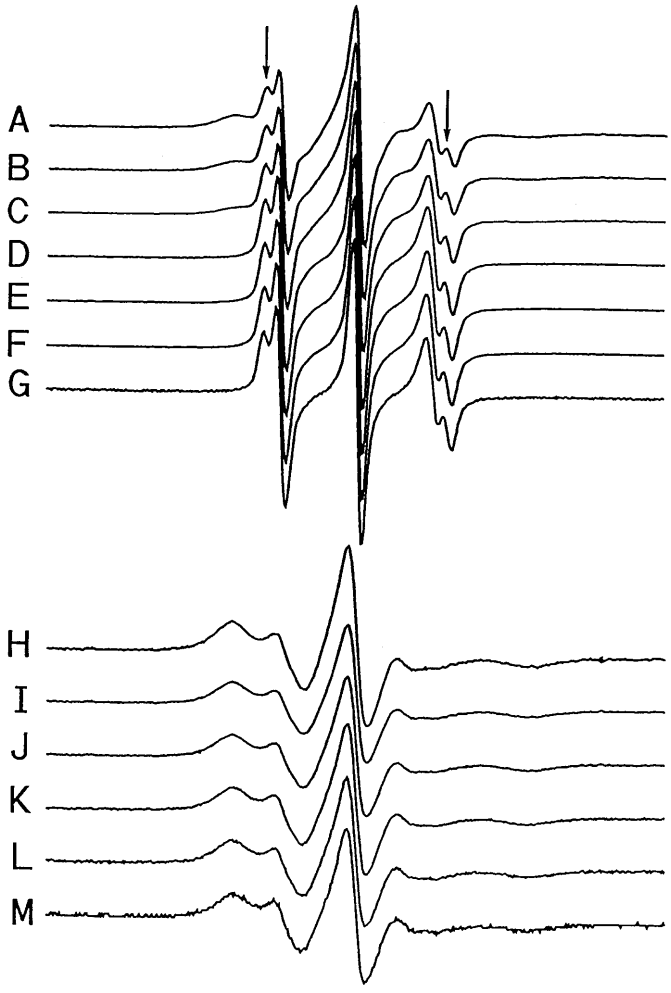

Fig. 5 EPR spectra of 16NPC in EYPC SUV containing varying amounts of FPI. The sharp triplet superimposed on the spectra is the TCC *x*-axis alignment marker and internal concentration standard. Mid-field of the spectra is 3351 G. The spectra were recorded at 293 K using a microwave power of 5 mW, a modulation amplitude of 2 G, a sweep time of 2 min and a time constant of 100 ms. *Upper:* peptide/lipid ratios: *A* 1/25, *B* 1/50, *C* 1/100, *D* 1/150, *E* 1/200, *F* 1/400, *G* control (recorded at 291 K). *Lower:* subtraction spectra: *H* A-G (×5), *I* B-G (×10), *J* C-G (×15), *K* D-G (×20), *L* E-G (×40), *M* F-G (×80)

tions and the C10–12 location of the spin-labelled N-terminus is compatible with the 41° tilt from the normal of the bilayer calculated for the 16-residue FP N-terminal helix by Brasseur et al. (1988) and Martin et al. (1996). It should be noted that Lüneberg et al. (1995) similarly found that the N-terminus of a spin-labelled influenza virus fusion peptide inserted into the hydrophobic core of EYPC vesicles and that at high P/L some of the peptide was exposed to the external medium. They did not, however, find increasing aggregation of their peptide with increasing P/L. However, because of the extensive probe/probe interaction, we were unable to obtain an estimate of the position of the N-terminus at P/Ls of 1/500 or 1/100, which more realistically correspond to the values at which fusion and other membrane perturbation effects by FP have been observed (Rafalski et al. 1990; Slepushkin et al. 1992; Nieva et al. 1994; Mobley et al. 1995; Pereira et al. 1997). In order to understand further the nature of the fusion peptide/lipid interaction at high P/Ls we obtained a series of EPR spectra of 16NPC with FPI in SUV. The measurement of the interaction between spin-labelled lipids and membrane-penetrant protein segments and peptides has been widely used to determine the nature of the association between lipids and proteins in membranes (Marsh 1989). In Fig. 5A–G are shown spectra of 16NPC at 293 K in SUV made from EYPC containing an increasing mole fraction of FPI. It can be seen that there is a relatively immobilised component in the spectra that increases with increasing P/L. Increasing amounts of the spectrum of the control SUV preparation recorded at 291 K were subtracted from the spectrum of each peptide-containing preparation to yield a series of spectra giving a clear end-point (Fig. 5H–M). Attempts were made to determine whether the presence of the peptide extensively perturbed the bulk lipid, as suggested by McIntyre et al. (1982), by subtracting the spectrum of the control SUV made at 286 K. In this operation it is assumed that the lower temperature spectrum would simulate that of bulk lipid whose motion had been restricted by long-range effects arising from the presence of the peptide. It was found that using the lower temperature spectrum did not lead to a clear end-point and it was impossible to obtain a well-behaved first integral with no negative excursions below the baseline (Jost and Griffith 1978). It was also found possible to simulate the spectra over the range of P/L mixtures used, as described by Davoust and Devaux (1982). The on and off rate constants for the P/L range 1/400–1/25 are given in Table 2. It was concluded, therefore, that long-range perturbation effects on the bulk lipid by the peptide at high P/L were negligible. The proportion of the slow motional component in each spectrum was therefore calculated by double integration and is plotted against the mole fraction of FPI in Fig. 6. It can be seen that the relationship is non-linear, fewer moles of lipid per

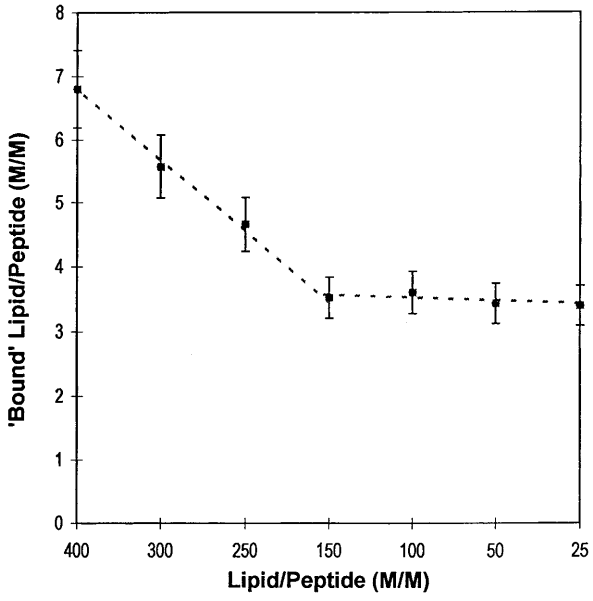

Fig. 6 Plot of proportion of ratio (M/M) of relatively immobilised spin-labelled phospholipid to FPI against FPI concentration. Each point is an average of three separate EPR experiments. Error bars show range

Table 2 On- and off-rate constants, t_f^{-1} and t_b^{-1}, respectively, for lipid exchange of 16NPC at the peptide lipid interface of FPI in EYPC as a function of P/L

P/L	t_f^{-1} (s^{-1})	t_b^{-1} (s^{-1})
1/400	7.1×10^{-6}	6.7×10^{-6}
1/300	6.8×10^{-6}	6.3×10^{-6}
1/200	6.5×10^{-6}	6.1×10^{-6}
1/150	6.7×10^{-6}	5.9×10^{-6}
1/100	6.3×10^{-6}	5.1×10^{-6}
1/50	6.1×10^{-6}	5.3×10^{-6}
1/25	5.9×10^{-6}	4.9×10^{-6}

Table 3 Spin-lattice relaxation times and chemical shift assignments for ^{13}C nuclei in EYPC SUV in the presence and absence of FPII[a]

Chemical shift (ppm)	Assignment[b]	NT_1 (s) EYPC	NT_1 (s) EYPC+FPII
59.7	$-N(CH_3)_3$	1.53	1.41
66.3	$-CH_2N-$	0.64	0.68
54.1	$-O-CH_2-$	0.64	0.56
62.5	glycerol$-CH_2-$	0.30	0.26
34.1	$-CH_2-CO_2-$	0.68	0.72
27.3	$-CH_2-\underline{C}H_2-CH=CH-$	0.96	0.86
129.7	$-CH=\underline{C}H-CH_2-CH_2-$	0.60	0.54
127.9	$-CH=CH-\underline{C}H_2-CH=CH-$	0.82	0.78
25.6	$-CH=\underline{C}H-CH_2-CH=CH-$	0.78	0.54
30.0	$-(CH_2)_n-$	1.00	0.86
32.0	$-\underline{C}H_2-CH_2-CH_3$	1.42	1.08
22.6	$-\underline{C}H_2-CH_3$	2.02	1.52

[a] Arranged in order of increasing distance of carbons from head group
[b] Assignments are those of Godici and Landsberger (1974) adjusted for external reference to DSS at 0.00 ppm rather than to CS_2 as reported in their paper

mole of peptide being perturbed at high mole fractions of the peptide.

A possible explanation of this result could be the formation of larger aggregates of FP1 at higher P/L. Another possibility could be that increasing amounts of peptide were located away from the hydrophobic core of the lipid bilayer probed by the 16NPC.

NMR : spin-lattice relaxation measurements

It is possible to determine the location of FPII with respect to EYPC using spin-lattice relaxation measurements on the ^{13}C nuclei of the lipid hydrocarbon chains by comparison of NT_1 values (where N corresponds to the number of hydrogens bonded to the carbon nucleus) in the presence and absence of spin-labelled peptide. The effects of adding the spin-labelled peptide, FP-II, on the spin-lattice relaxation times of the resolvable ^{13}C nuclei in EYPC are given in Table 3. The assignments are shown in order of their approximate position in the fatty acyl chain.

For EYPC in the absence of peptide, NT_1 values follow a similar trend to that observed by Godici and Landsberger (1974). A general increase in NT_1 values from the carbonyl group to the terminal CH_3 indicates an increase in motion along the fatty acid chain. However, as noted by Godici and Landsberger (1974), reduced NT_1 values are observed in the vicinity of the double bonds, reflecting a lack of rotational freedom at these sites. An increase in motional freedom is also observed going from the relatively immobile glycerol backbone to the choline group. The addition of the spin-labelled peptide (P/L 100) has little effect on the spin-lattice relaxation of carbon atoms in the upper region of the lipid bilayer (average 1.2% decrease), indicating that FPII does not interact with the head group. However, a significant decrease in NT_1 values is observed along the fatty acid chain (average 12.3%) and the effect is enhanced towards the terminal CH_3 group. This indicates that at this P/L a significant fraction of FPII is located with its amino-terminus towards the mid-region of bilayer.

Solid state NMR

To obtain information on the state of aggregation of the peptide that we had observed at high P/L spectra of FPII we carried out SSNMR studies on FPI_a in DTPC multilayers. Although this system is physically and chemically different from the EYPC SUV, it still consists of neutral lipid but in the case of multilayers the lipid bilayer is no longer curved. The lipid is fully hydrated (50% w/w water) but there is no excess water present (Simon et al. 1995). Over P/Ls of 1/10, 1/20 and 1/30, we obtained broad spectra at both the 0° and 90° orientations (Fig. 7), whereas the lipid signal showed an orientation dependence. These results suggest that the peptide was aggregated at these P/L values. The spin-lattice relaxation times for ^{13}C in this system are given in Table 4 and the ^{13}P relaxation times for the lipid in the presence of the peptide are given in Table 5.

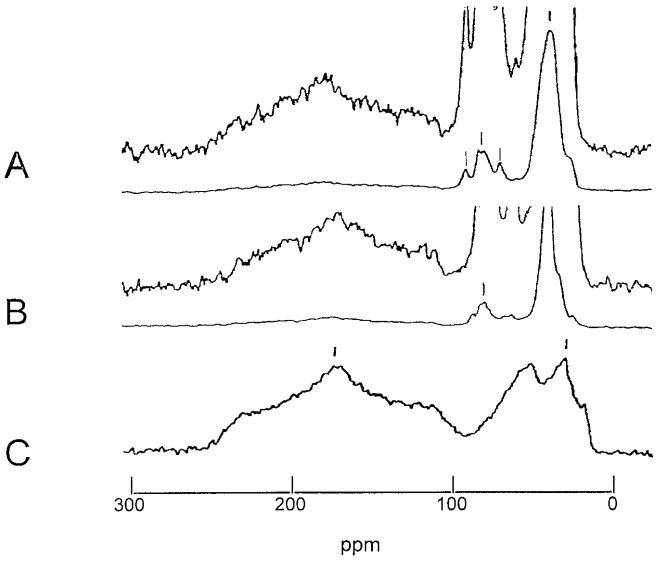

Fig. 7 Solid state ^{13}C spectra of $FP1_a$ in aligned multilayers in DTPC and as a solid powder. Water content 50%, temperature 303 K, P/L 1/20, other conditions as given in Materials and methods. *A* alignment with bilayer normal at 0°C; *B* alignment with bilayer normal at 90°; *C* powder

Table 4 Proton relaxation times for FPI_a in DTPC and as a dry powder at 303 K [a]

Sample	T_1 (ms)	$T_{1\rho}$ (ms)	$T_1/T_{1\rho}$	Orientation
DTPC	285	27.0	11	aligned
FPI_a in DTPC (1/30)	425	9.4	45	aligned
FPI_a in DTPC (1/20)	500	8	63	aligned
FPI_a in DTPC (1/12)	443	5.8	92	aligned
FPI_a	584	10.0	58	powder

[a] Measured via ^{13}C C–P

The ratio of $T_1/T_{1\rho}$ of the lipid methylenes increased from 11 to 92 as the amount of peptide increased, indicating an increase in the intensity of low-frequency motion of the lipid molecules. However, the phosphorus relaxation from the lipid headgroups had a lesser change upon the addition of FPI_a. The lipid remained in a lamellar phase but was less well aligned in the presence of the peptide. These data suggest that the aggregated peptide does not form a continuum or large aggregates phase-separated from the multilayers but, rather, exists as discret oligomers. In summary, the peptide was all lipid-associated and it formed oligomers which affected the motion of the lipid chains and disrupted the lipid alignment. The peptide was aggregated and did not show any orientation dependence or long axis reorientation, as indicated by the carbonyl powder pattern (Fig. 7). Membrane-interactive polypeptides, such as gramicidin A (Cornell et al. 1988) and melittin, exhibit narrow carbonyl spectra and a chemical shift that is dependent on the orientation of the bilayer normal to the magnetic field, at the same P/L ratios in DTPC multilayers. FPI_a, however, in multilayers is immobile under these conditions but influences the mobility of the lipid molecules in the same way (Smith et al. 1992). It is interesting that the peptide appears to be aggregated in both aligned and non-aligned multilayers and SUVs made from phosphatdylcholine lipids.

Table 5 Comparison of ^{31}P relaxation times for aligned and powdered samples of FPI_a in DTPC at 303 K

Sample	T_2 (ms)	$T_{1\rho}$ (CP) (ms)	T_1 (CP) (ms)	T_1 (ms)	Orientation
Aligned sample 50% w/w H_2O					
DTPC	2.4	2.1	415	512	aligned
FPI_a + DTPC (1/20)	1.7	2.0	411	422	aligned
Powder sample in 50% w/w H_2O					
FPI_a + DTPC	1.5	2.4	490	426	powder

Conclusions

Although we must be cautious in drawing conclusions from our diverse experimental approaches, our results suggest that it is possible for FPI to interact with neutral lipid vesicles without producing the gross outcomes of fusion and leakage, even at high P/L. Since, apparently, the bilayer in our SUV remains intact, our data may reflect the situation obtaining in the initial phase of the destabilisation of more complex membranes by FPI.

The density gradient experiments show that the peptide is associated with the lipid, even at high P/L. The peptide forms aggregates at high P/L, as shown by the EPR experiments with FPII and by the SSNMR data. Although the latter technique employs planar lipid multilayers at low levels of hydration, it has proved successful in elucidating the structure of other membrane-associated peptides, notably gramicidin (Cornell et al. 1988). That the aggregation is found in a constrained planar system argues against it being an artefact arising from the nature of the highly curved bilayer of the SUV. By the same token, the aggregation is also unlikely to be an artefact of employing a spin-labelled peptide. That the aggregation was observed at much lower P/L in the EPR experiments might merely argue for the technique's sensitivity compared with other methods. It should be noted that aggregation of FPII had already been observed by EPR at comparably low P/L in red cell ghosts and multilamellar vesicles made from ghost lipids (Gordon et al. 1992).

The spin-lattice relaxation experiments indicate that at a P/L of 1/100 most of the N-terminus of the peptide is associated with the C10–C12 region of the lipid. There was no observable effect on the T_1 of the choline carbon nuclei at the P/L used, suggesting that very little, if any, of the peptide N-terminus was exposed to the lipid head groups. Since, at this P/L, FPI is haemolytic (Mobley et al. 1992) and fuses red cell ghosts (Mobley et al. 1995), it is likely that the intramembrane aggregates play a role in the fusion and lytic behaviour of FPI. They are, therefore, worthy of investigation in a range of membrane systems by other techniques such as low angle X-ray scattering (Simon et al. 1995).

References

Altenbach C, Hubbell WL (1988) The aggregation state of spin-labeled melittin in solution and bound to phospholipid membranes: evidence that membrane-bound melittin is monomeric. Proteins Struct Funct Genet 3: 230–242

Andrade M, Chacon P, Merelo J, Moran F (1993) Evaluation of secondary structure of proteins from UV circular dichroism spectra using an unsupervised learning neural network. Protein Eng 6: 383–390

Brasseur R, Cornet B, Burny A, Vandenbranden M, Ruysschaert J (1988) Mode of insertion into a lipid membrane of the N-terminal HIV gp41 peptide segment AIDS Res Hum Retroviruses 4: 83–90

Brasseur R, Vandenbranden M, Cornet B, Burny A, Ruysschaert J-M (1990) Orientation into the lipid bilayer of an asymmetric amphipathic helical peptide located at the *N*-terminus of viral fusion proteins. Biochim Biophys Acta 1029: 267–273

Chang D, Cheng S, Chien W (1997) The amino-terminal fusion domain of human immunodeficiency virus type 1 gp41 inserts into the sodium dodecyl sulfate micelle primarily as α-helix with a conserved glycine at the micelle-water interface. J Virol 71: 6593– 6602

Cornell B, Separovic F, Baldassi A, Smith R (1988) Conformation and orientation of gramicidin A in oriented phospholipid bilayers measured by solid state carbon-13 NMR. Biophys J 53: 67–76

Davoust J, Devaux P (1982) Simulation of electron spin resonance spectra of spin-labeled fatty acids attached to the boundary of an intrinsic membrane protein. A chemical exchange model. J Magn Reson 48: 475–486

Doms R, Earl P, Chakrabarti S, Moss B (1990) Human immunodeficiency virus types 1 and 2 and simian immunodeficiency virus *env* proteins possess a functionally conserved assembly domain. J Virol 64: 3537–3540

Ellena J, Blazing M, McNamee M (1983) Lipid-protein interactions in reconstituted membranes containing acetylcholine receptor. Biochemistry 22: 5523–5534

Ellens H, Bentz J Szoka F (1985) H^+- and Ca^{2+}-induced fusion and destabilization of liposomes. Biochemistry 24: 3099–3016

Felser J, Klimkait T, Silver J (1989) A syncytia assay for human immunodeficiency virus type-I (HIV-1) envelope protein and its use in studying HIV-1 mutations. Virology 170: 566–570

Freed E, Myers D, Risser R (1990) Characterization of the fusion domain of the human immunodeficiency virus type 1 envelope glycoprotein gp41. Proc Natl Acad Sci USA 87: 4650–4654

Gaffney BJ (1974) Spin-label measurements in membranes. Methods Enzymol 32B: 161–198

Godici PE, Landsberger FR (1974) The dynamic structure of lipid membranes. A ^{13}C nuclear magnetic resonance study using spin labels. Biochemistry 13: 362–368

Gordon LM, Curtain CC (1988) Electron spin resonance analysis of model and biological membranes. In: Aloia RC, Curtain CC, Gordon LM (eds) Advances in membrane fluidity 1: methods for studying membrane fluidity. Liss, New York, pp 25–89

Gordon LM, Curtain CC, Zhong Y, Kirkpatrick A, Mobley PW, Waring A (1992) The amino terminal peptide of HIV-I glycoprotein 41 interacts with human erythrocyte membranes: peptide conformation, orientation and aggregation. Biochim Biophys Acta 1139: 257–274

Jost P, Griffith O (1978) The spin-labeling technique. Methods Enzymol 49: 369–418

Keith A, Horvat D, Snipes W (1974) Spectral characterization of ^{14}N spin labels. Chem Phys Lipids 13: 49–62

Levy G, Lichter R, Nelson G (1980) Carbon-13 nuclear magnetic resonance spectroscopy, 2nd edn. Wiley, New York, pp 211–246

Lüneberg J, Martin I, Nüssler F, Ruysschaert J-M, Herrmann A (1995) Structure and topology of the influenza virus fusion peptide in lipid bilayers J Biol Chem 270: 27606–27614

McIntyre J, Samson P, Brenner S, Dalton L, Fleischer S (1982) EPR studies of the motional characteristics of the phospholipid in functionally reconstituted sarcoplasmic reticulum membranes. Biophys J 37: 53–56

Marsh D (1989) Experimental methods in spin-label spectral analysis. In: Berliner L, Reuben J (eds) Biological magnetic resonance 8: spin labeling theory and applications. Plenum Press, New York, pp 255–303

Martin I, Dubois M-C, Saermark T, Ruysschaert J-M (1992) Apolipoprotein A-1 interacts with the N-terminal fusogenic domains of SIV (simian immunodeficiency virus) gp32 and HIV (human immunodeficiency virus) gp41: implications in viral entry. Biochim Biophys Res Commun 186: 95–101

Martin I, Schaal H, Scheid A, Ruysschaert JM (1996) Lipid membrane fusion induced by the human immunodeficiency virus type 1 gp41 N-terminal extremity is determined by its orientation in the lipid bilayer. J Virol 70: 298–304

Merelo JJ, Andrade MA, Prieto A, Moran F (1994) Proteinotopic feature maps. Neurocomputing 6: 1–12

Mobley PW, Curtain CC, Kirkpatrick A, Rostamkhani M, Waring AJ, Gordon LM (1992) The amino-terminal peptide of HIV-1 glycoprotein 41 lyses human erythrocytes and $CD4^+$ lymphocytes. Biochim Biophys Acta 1139: 251–256

Mobley PW, Lee H-F, Curtain CC, Kirkpatrick A, Waring AJ, Gordon LM (1995) The amino-terminal peptide of HIV-1 glycoprotein fuses human erythrocytes. Biochim Biophys Acta 1271: 304–314

Myers G, Korber B, Berzofsky JA, Smith RF, Pavalakis GN (eds) (1991) Human Retroviruses and AIDS 1991: a compilation and analysis of nucleic acid and amino acid sequences. Los Alamos National Laboratory, Los Alamos, NM, pp 11–81

Nieva JL, Nir S, Muga A, Goni FM, Wilschut J (1994) Interaction of the HIV-1 fusion peptide with phospholipid vesicles: different structural requirements for fusion and leakage. Biochemistry 29: 7917–7922

Op den Kamp JF (1979) Lipid asymmetry in membranes. Annu Rev Biochem 48: 47–71

Peirira FB, Goni FM, Muga A, Nieva JL (1997) Permeabilization and fusion of uncharged lipid vesicles induced by the HIV-1 fusion peptide adopting an extended conformation – dose and sequence effects. Biophys J 73: 1977–1986

Pines A, Gibby MG, Waugh JS (1973) Proton enhanced NMR of dilute spins in solids. J Chem Phys 59: 569–590

Pinter A, Honnen WJ, Tilley SA, Bona C, Zaghounani H, Gorney MK, Zolla-Pazner S (1989) Oligomeric structure of gp41, the transmembrane protein of human immunodeficiency virus type 1. J Virol 63: 2674–2679

Rafalski M, Lear JD, DeGrado WF (1990) Phospholipid interactions of synthetic peptides representing the N-terminus of HVI gp41. Biochemistry 9: 7917–7922

Rothman JE, Lenard J (1977) Membrane asymmetry. Science 195: 743–753

Ruocco MJ, Makriyannis A, Siminovitch DJ, Griffin RG (1985) Deuterium NMR investigation of ether- and ester-linked phosphatidylcholine bilayers. Biochemistry 24: 4844–4851

Schneider DJ, Freed JL (1989) In: Berliner LJ, Reuben J (eds) Biological magnetic resonance 8: spin labeling theory and applications. Plenum Press, New York, pp 1–76

Simon SA, Advani S, McIntosh TJ (1995) Temperature dependence of the repulsive pressure between phosphatidylcholine bilayers. Biophys J 69: 1473–1482

Slepushkin VA, Melikyan GB, Sidorova MS, Chumakov VM, Andreev SM, Manulyan RA, Karamov EV (1990) Interaction of human immunodeficiency virus (HIV-1) fusion peptides with artificial lipid membranes. Biochem Biophys Res Commun 172: 952–957

Struck DK, Hoekstra D, Pagano RE (1981) Use of resonance energy transfer to monitor membrane fusion. Biochemistry 20: 4093–4099

White J, Killian M, Helinius A (1983) Membrane fusion proteins of enveloped animal viruses. Q Rev Biophys 16: 151–195

Yeagle PL, Epand RM, Richardson CD, Flanagan TD (1991) Effects of "fusion peptide" from measles virus on the structure of N-methyl dioleoylphosphatidylethanolamine membranes and their fusion with Sendai virus. Biochim Biophys Acta 1065: 49–53